Supporting Information

Content:

Additional experimental procedures.

Synthesis of 10,10-dichlorophenoxatellurine, (PT)Cl_2.[27] Diphenyl ether (7.00 g, 41.2 mmol) and tellurium tetrachloride (11.1 g, 41.2 mmol) were set into a flask with an air-condenser, carrying a moisture guard-tube and heated at 150°C for two hours and at 200°C for four hours, while hydrogen chloride was evolved. The cooled melt was ground and stirred with diethyl ether. After filtration the residue was stirred with acetone and filtered again. The solvent was evaporated and left crude (PT)Cl_2 (14.4 g, 39.3 mmol) that was used without further purification in the next step. A small amount of the crude product was recrystallized from acetonitrile to give orange-brown needles of (PT)Cl_2·1/2 MeCN.

^{1}H-NMR (360 MHz, d_6-acetone): δ = 8.04 - 7.73 (m, 12H, C_{Ar}-**H**) ppm. ^{13}C-NMR (90 MHz, Acetone-d_6): δ = 150.5, 133.3, 132.8, 124.7, 119.1 (**C**$_{Ar}$), 117.9 (C_{Ar}-**C**H-Te), ^{125}Te-NMR (110 MHz, d_6-acetone): δ = 594.4 ppm.

Synthesis of Phenoxatellurine (PT). A mixture of (PT)Cl_2 (2.00 g, 5.45 mmol) sodium sulfide nonahydrate (3.93 g, 16.35 mmol) were heated to 100°C for 15 minutes. After cooling to room temperature the solid was stirred with diethyl ether and washed with water. The organic layer was then separated and dried with magnesium sulfate. Evaporation of the ether left a dark reddish-brown solid, which on further purification by sublimation to give yellow spear-like needles of PT (1.60 g, 5.41 mmol, 99 %; Mp. 77°C. (78 - 79°C[27]))

^{1}H-NMR (360 MHz, $CDCl_3$): δ = 7.68 - 7.06 (m, 12H, C_{Ar}-**H**) ppm. ^{13}C-NMR (90 MHz, $CDCl_3$): δ = 165.8, 135.2, 129.4, 125.8, 119.9 (**C**$_{Ar}$), 106.6 (C_{Ar}-**C**H-Te), (C_{Ar}-**C**H-O) ppm. ^{125}Te-NMR (110 MHz, $CDCl_3$): δ = 420.0 ppm. MS (EI, 70 eV, 200 °C): m/z = 298 [M^+], 168 [M-Te]$^+$, 139 [M-Te-CHO]$^+$. UV/VIS (CH_2Cl_2): λ_{max} = 279 nm, 343 nm.

Table S1. Crystal data and structure refinement of $PtCl_2 \cdot 1/2$ NCMe and PT.

	$PTCl_2 \cdot 1/2$ NCMe	PT[#]
Formula	$C_{26}H_{19}Cl_4NO_2Te_2$	$C_{12}H_8OTe$
Formula weight, g mol^{-1}	774.42	295.78
Crystal system	monoclinic	orthorhombic
Crystal size, mm	0.08 × 0.08 × 0.07	0.09 × 0.07 × 0.03
Space group	*C*2/c	$P2_12_12_1$
a, Å	27.070(2)	5.9407(2)
b, Å	13.247(1)	8.0196(3)
c, Å	7.4254(7)	20.6459(6)
α, º	90	90
β, º	94.945(3)	90
γ, º	90	90
V, Å^3	2652.8(4)	983.61(6)
Z	4	4
ρ_{calcd}, Mg m^{-3}	1.939	1.997
μ (Mo $K\alpha$), mm^{-1}	2.628	2.983
F(000)	1480	560
θ range, deg	2.74 to 35.03	2.62 to 27.50
Index ranges	$-31 \le h \le 32$	$-10 \le h \le 10$
	$-10 \le k \le 15$	$-11 \le k \le 14$
	$-7 \le l \le 8$	$-36 \le l \le 29$
No. of reflns collected	4974	13802
Completeness to θ_{max}	94.2%	99.0%
No. indep. Reflns	1941	5780
No. obsd reflns with ($I>2\sigma(I)$)	1703	5309
No. refined params	161	127
GooF (F^2)	1.143	1.038
R_1 (F) ($I > 2\sigma(I)$)	0.0329	0.0258
wR_2 (F^2) (all data)	0.0871	0.0490
Largest diff peak/hole, e Å^{-3}	0.942 / –0.526	0.989 / –0.424
CCDC number	1895457	1895458

[#] Reinvestigation with inclusion of hydrogen atoms.[37]

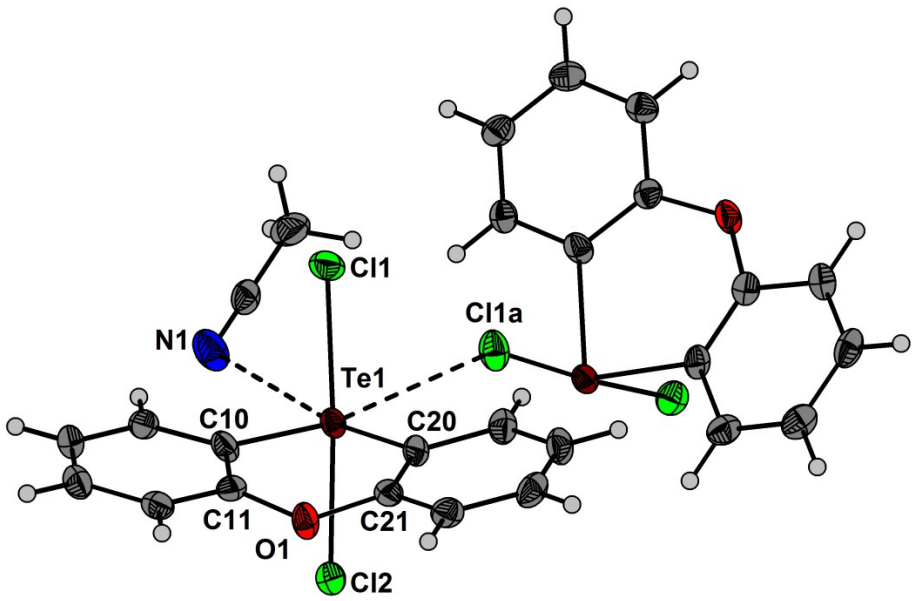

Figure S1. Molecular structure of (PT)Cl_2·1/2 NCMe showing 50% probability ellipsoids

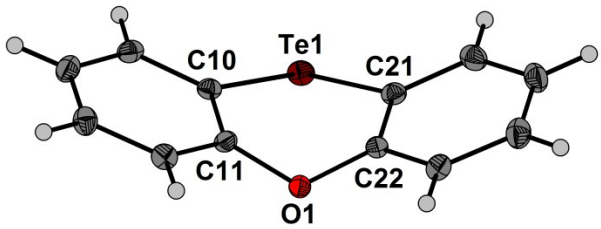

Figure S2. Molecular structure of PT showing 50% probability ellipsoids

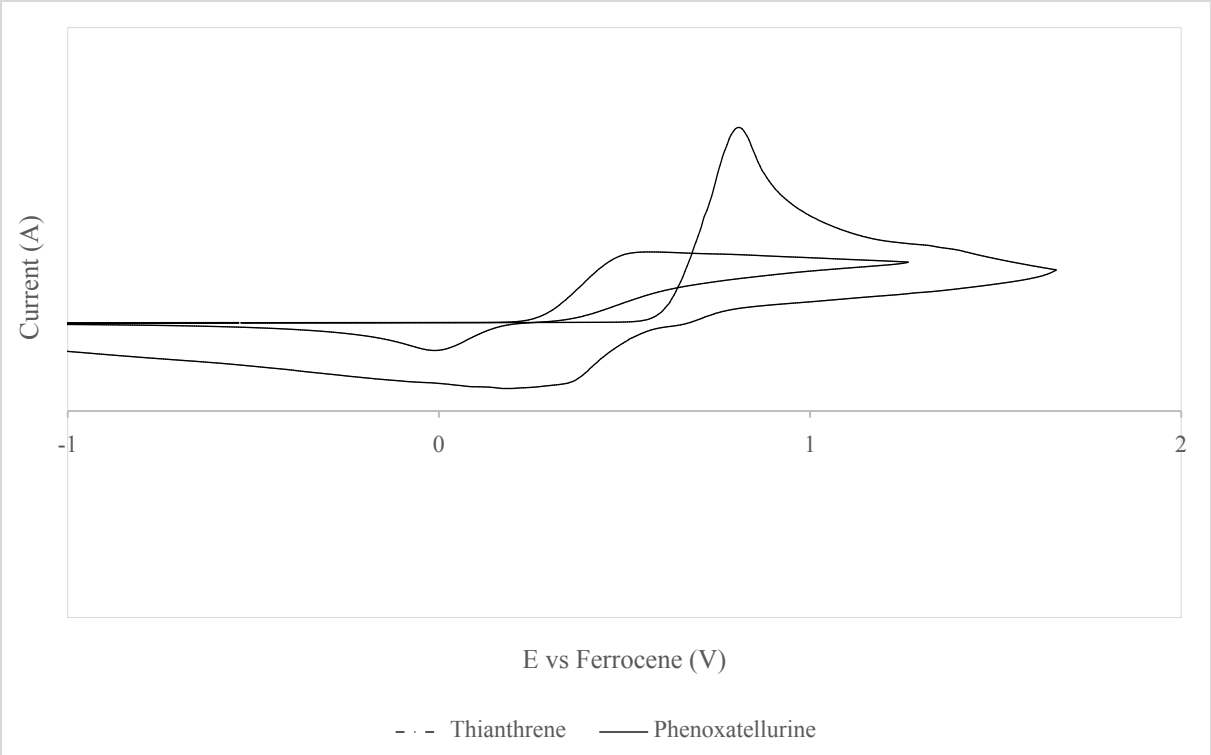

Figure S3. Cyclic voltammetry measurement of phenoxatellurine (5.5 mg/mL) and thianthrene (5.7 mg/mL), conducting salt (0.1 M Bu_4NPF_6) in dichloromethane. The peak potential data for the two scans are:

E_{p1}^{a} TA	+0.81 V	E_{p1}^{a} PT	+0.52 V
E_{p1}^{c} TA	+0.34 V	E_{p1}^{c} PT -	+0.01 V

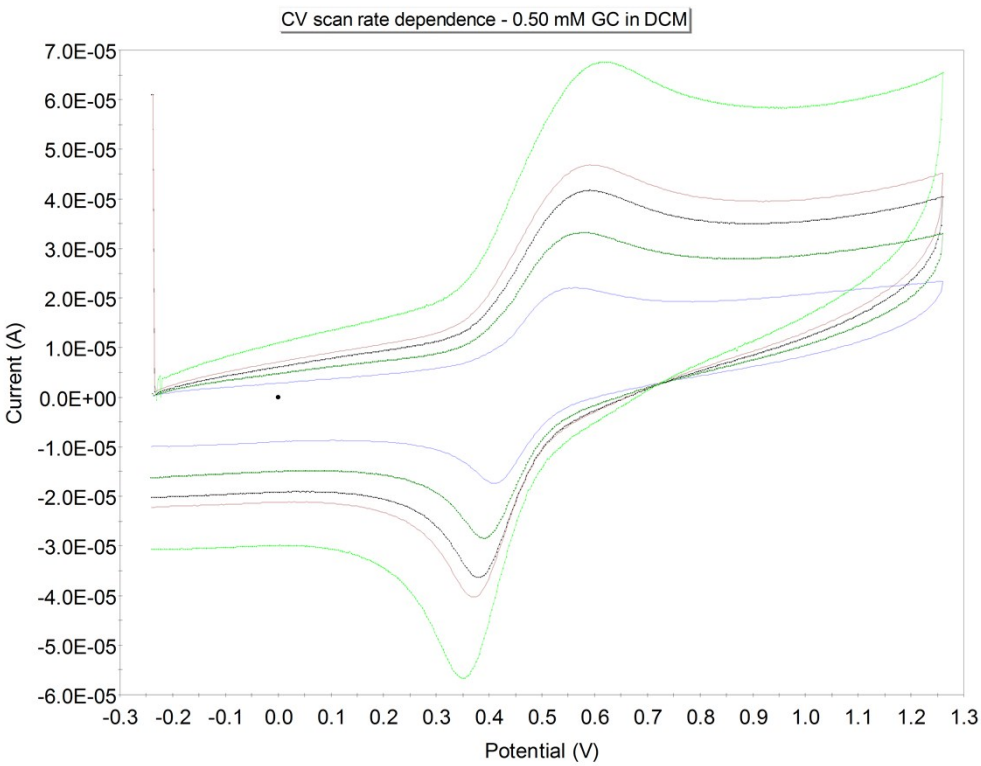

Figure S4. Scan rate dependence (0.2, 0.5, 0.8, 1.0 2.0 V/s) for CVs of PT in anodic scans through the first oxidation process in $CH_2Cl_2/[^nBu_4N][PF_6]$ at a GC electrode. The ΔE^{a-c} (peak separation) varies as: 0.2: 152; 0.5: 189; 0.8, 200; 1.0, 228; 2.0, 262 mV.

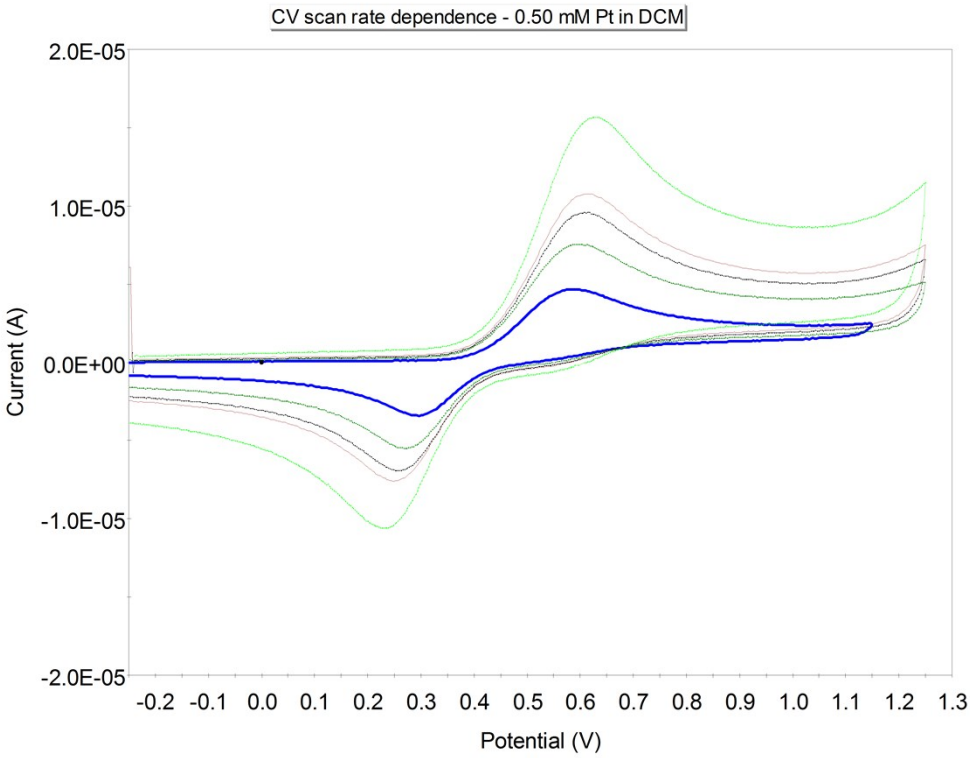

Figure S5. Scan rate dependence (0.2, 0.5, 0.8, 1.0 2.0 V/s) for CVs of PT in anodic scans through the first oxidation process in $CH_2Cl_2/[^nBu_4N][PF_6]$ at a Pt electrode. The ΔE^{a-c} (peak separation) varies as: 0.2: 292; 0.5: 327; 0.8, 355; 1.0, 363; 2.0, 394 mV.

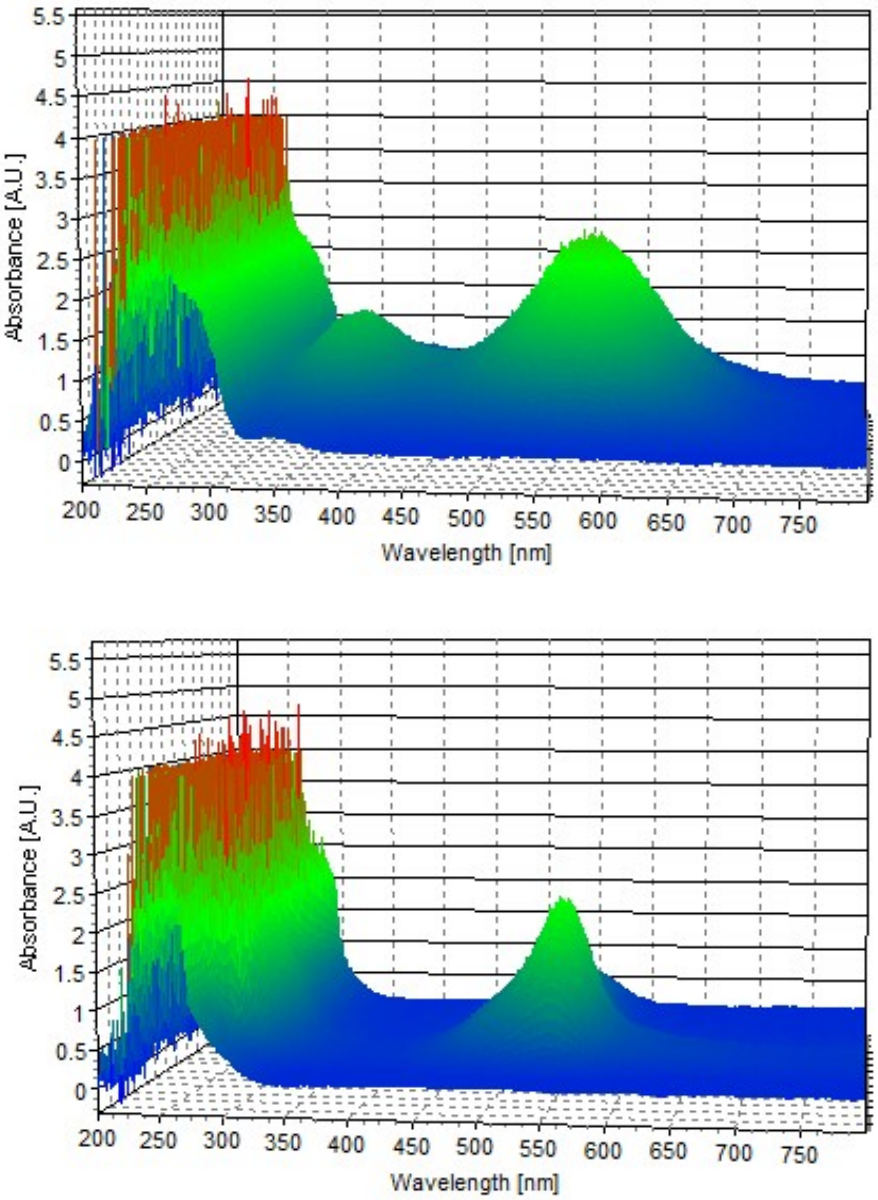

Figure S6. UV-Vis Spectroelectrochemical measurement of PT (top) and TA (bottom).

Table S2. Simulated isotropic EPR spectrum of $PT^{\bullet+}$ from DFT calculations

EPR Simulation: phenoxytellurine radical cation

From: Farzin_1_p1_opt UB3PW91 6-311+G(2df,p) // Te = ? Doublet

Isotropic Fermi Contact Couplings

	Atom	Abundanc	a.u.	MegaHert	Gauss	|Gauss|
16	H(1)	99.98	-0.00083	-3.72438	-1.32895	1.32895
20	H(1)	99.98	-0.00076	-3.38561	-1.20807	1.20807
17	H(1)	99.98	-0.00056	-2.50503	-0.89386	0.89386
21	H(1)	99.98	-0.00055	-2.43668	-0.86947	0.86947
15	H(1)	99.98	0.00012	0.53236	0.18996	0.18996
19	H(1)	99.98	0.0001	0.45473	0.16226	0.16226
18	H(1)	99.98	-0.00006	-0.26259	-0.0937	0.0937
22	H(1)	99.98	-0.00005	-0.23849	-0.0851	0.0851
1	Te(125	7.07	-0.00015	0.2137	0.07625	0.07625
5	C(13)	1.109	-0.00389	-4.37657	-1.56167	1.56167
11	C(13)	1.109	-0.00368	-4.13592	-1.4758	1.4758
3	C(13)	1.109	-0.00324	-3.64259	-1.29977	1.29977
9	C(13)	1.109	-0.00313	-3.52181	-1.25667	1.25667
8	C(13)	1.109	-0.00249	-2.79998	-0.9991	0.9991
14	C(13)	1.109	-0.00244	-2.74417	-0.97919	0.97919
10	C(13)	1.109	-0.00157	-1.76825	-0.63096	0.63096
4	C(13)	1.109	-0.00137	-1.54085	-0.54981	0.54981
6	C(13)	1.109	0.00085	0.95299	0.34005	0.34005
12	C(13)	1.109	0.00065	0.73138	0.26097	0.26097
7	C(13)	1.109	-0.00049	-0.54619	-0.19489	0.19489
13	C(13)	1.109	-0.00045	-0.50345	-0.17964	0.17964
2	O(17)	0.0373	0.01738	-10.5349	-3.75912	3.75912

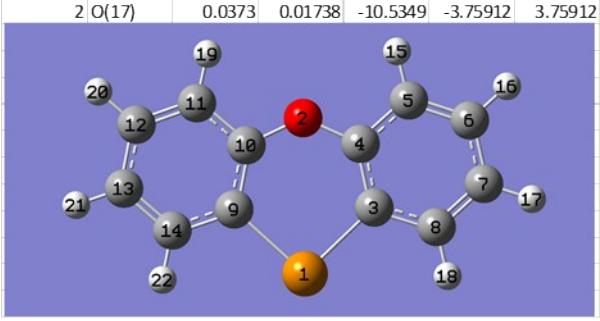

Simulaed EPR spectrum of the phenoxytellurine radical from DFT

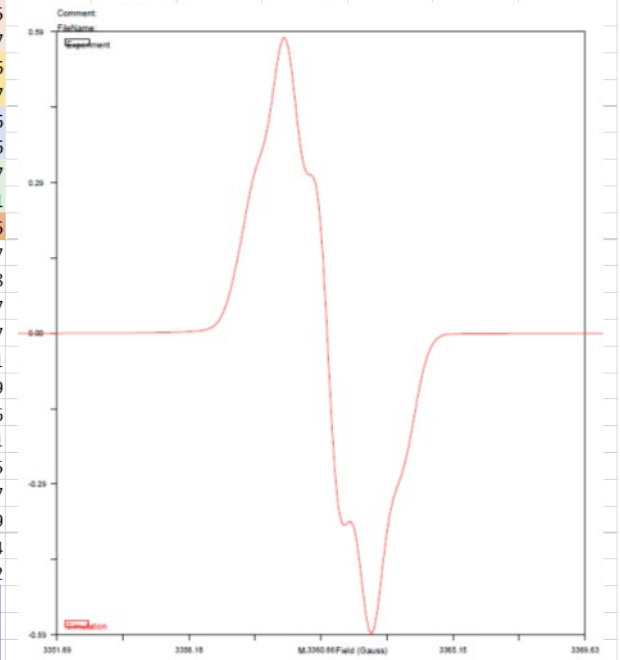

For sake of comparison, the same 0.5 G LW is used here for the simulation
In reality, we expect the strong spin-orbit coupling of Te to significantly
increase the LW of this radical compared to that of the thianthrene.
This is expected to elminate any resolvable hyperfine splitting in the signal.

Table S3. Simulated isotropic EPR spectrum of $TA^{\bullet+}$ from DFT calculations

EPR Simulation: thianthrene radical cation

From: 17_SS_1_p1_m1_gas_opt UB3PW91 6-311+G(2df,p) Doublet

Isotropic Fermi Contact Couplings

	Atom	Abundanc	a.u.	MegaHert	Gauss	|Gauss|
20	H(1)	99.98	-0.00111	-4.97666	-1.77579	1.77579
17	H(1)	99.98	-0.00111	-4.97552	-1.77539	1.77539
21	H(1)	99.98	-0.00111	-4.97329	-1.77459	1.77459
16	H(1)	99.98	-0.00111	-4.97315	-1.77454	1.77454
15	H(1)	99.98	-0.00018	-0.80997	-0.28902	0.28902
22	H(1)	99.98	-0.00018	-0.80956	-0.28887	0.28887
18	H(1)	99.98	-0.00018	-0.80883	-0.28861	0.28861
19	H(1)	99.98	-0.00018	-0.80683	-0.2879	0.2879
10	C(13)	1.109	-0.00377	-4.23822	-1.5123	1.5123
7	C(13)	1.109	-0.00377	-4.2356	-1.51137	1.51137
13	C(13)	1.109	-0.00377	-4.23354	-1.51063	1.51063
4	C(13)	1.109	-0.00376	-4.23231	-1.51019	1.51019
11	C(13)	1.109	0.00082	0.9223	0.3291	0.3291
6	C(13)	1.109	0.00082	0.92091	0.3286	0.3286
12	C(13)	1.109	0.00082	0.91847	0.32773	0.32773
5	C(13)	1.109	0.00082	0.91808	0.32759	0.32759
3	C(13)	1.109	-0.00049	-0.55045	-0.19641	0.19641
14	C(13)	1.109	-0.00049	-0.54762	-0.1954	0.1954
8	C(13)	1.109	-0.00048	-0.54364	-0.19398	0.19398
9	C(13)	1.109	-0.00048	-0.54088	-0.193	0.193
2	S(33)	0.76	0.04978	17.09676	6.10055	6.10055
1	S(33)	0.76	0.04978	17.0964	6.10042	6.10042

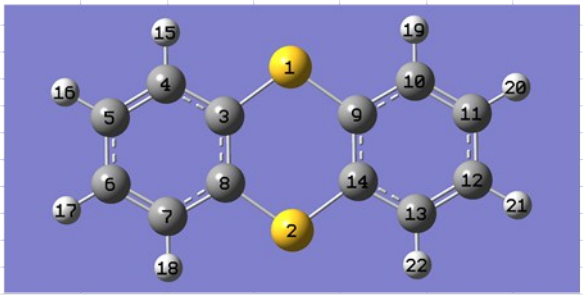

Simulated EPR spectrum of the thianthrene radical from DFT

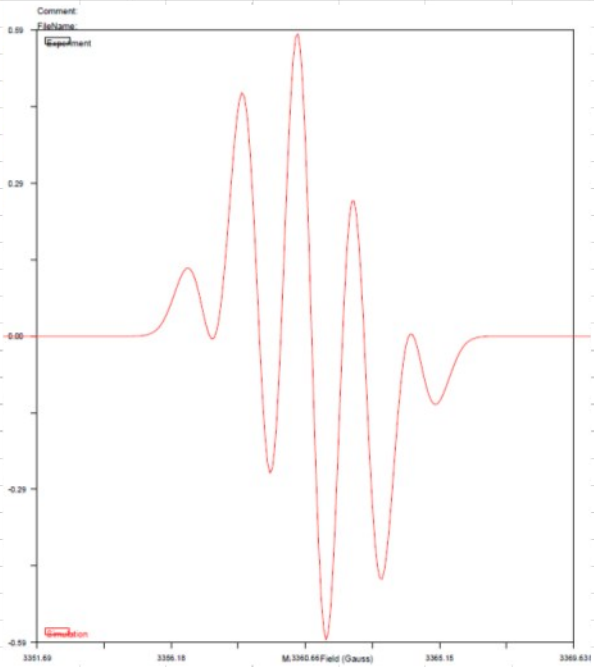

Note that the linewidth is merely an arbitrary value, and is likely too too narrow. The value here is 0.5 Gauss for a Laurentian function.